Int. J. Electrochem. Sci., 10 **(2015)** 6517 - 6526

International Journal of
ELECTROCHEMICAL
SCIENCE
www.electrochemsci.org

Formation and Characterization of the High Precision Nanoscale Thin Film Resistors on Radio Frequency Application

Huei Yu Huang[1], *Chia-Yu Wu*[2,3], *Chi-Chang Wu*[4,*]

[1]Department of Dentistry, Taipei Medical University-Shuang Ho Hospital, New Taipei City, Taiwan
[2] Department of Dentistry, Taipei Medical University Hospital, Taipei, Taiwan
[3] School of Dentistry, College of Oral Medicine, Taipei Medical University, Taipei, Taiwan
[4]Graduate Institute of Biomedical Materials and Tissue Engineering, College of Oral Medicine, Taipei Medical University, Taipei, Taiwan
[*]E-mail: half1997tainan@hotmail.com

Received: 11 May 2015 / *Accepted:* 29 May 2015 / *Published:* 24 June 2015

In this paper, a high-precision tantalum nitride thin film resistor was fabricated using a novel plasma ion etching method. Sheet resistance and x-ray spectra confirmed that the composition and crystalline lattice of the tantalum nitride film varied upon different nitrogen flow ratios of sputtering. To obtain a good performance, we proposed a novel two-step etching process for the fabrication of tantalum nitride thin film resistor, that is, firstly etched using a Cl_2 plasma for the purpose of sharp profile and fast etching rate, and followed by a Cl_2/O_2 gas mixture plasma to get a better etching selectivity. The temperature coefficient of resistance of the tantalum nitride thin film resistor showed that the temperature-related disturbance increased upon increasing the nitrogen composition of device. The temperature-related stability of the thin film resistor was further improved by post-deposited ammonia plasma treatment. The flicker noise, measured at frequency from 1 to 100k Hz, also showed that the current noise depended on the nitrogen composition of the thin film resistor. The characteristic of radio frequency dependent resistance, which was measured ranging from 1 to 20 GHz and extracted by two-ported S parameter and telegrapher's transmission line model, also showed that the stability of tantalum nitride thin film resistor decreased upon increasing the nitrogen composition.

Keywords: tantalum nitride, thin film resistor, plasma ion etching, temperature coefficient of resistance, flicker noise

1. INTRODUCTION

The dramatic increase in wired and wireless communications in recent years has demanded the need for high quality and precision nanoscaled integrated passive components for analog and mixed

signal applications [1, 2]. The integrated nanoscaled passive components provide efficient circuit miniaturization while maintaining high performance and assembly costs reduction [3, 4]. The inclusion of stable and precise nanoscaled on-chip passive devices is still a challenge for current and future interconnect architectures. This request for high-quality and high-precision integrated passive devices is mainly driven from the demand of advanced high frequency and system-on-a-chip (SOC) applications [5].

Precision nanoscaled thin film resistors (TFR) are widely used in analog and mixed signal circuits and advanced SOC applications [6, 7]. TFR nanodevice is one of the important passive elements in the integrated circuits. The properties of TFR devices must conform to the requests of easy fabrication, suitable resistance range, stable with both operating temperature and frequency, and low flicker noise.

Tantalum and its nitrogen-doped compound alloys have been used extensively as a candidate material of diffusion barrier in copper metallization system due to its high thermal stability. Incorporating with the nitrogen and oxygen during reactively sputtering, the resistances of the tantalum based nanoscaled thin films can be easily adjusted and optimized [8, 9]. Tantalum nitride (TaN_x) is a refractory metal alloy and able to sustain a thermal treatment up to 1400 ^oC without degradation. The range of resistivity of the TaN_x thin film can be as wide as 200 to 15000 □□-cm simply by using reactively sputtering method [10, 11]. The excellent properties of the TaN_x alloy demonstrate that it is potentially a candidate material as the advanced precision thin film resistor.

Although the good thermal stability and easy fabrication of the TaN_x nanoscaled thin film resistor, the temperature and frequency dependent stabilities are also important concerns for the advanced radio frequency and SOC applications [12]. However, there is little literature in studying those issues thoroughly. In this work, the formation and characterization of the TaN_x nanoscaled thin films resistors were studied. TaN_x nanosclaed thin films were deposited at various nitrogen flow ratios of reactive sputtering. The high-precision TaN_x nanoscaled thin film resistor was pattern by using lithography and plasma ion etching system. To inspect the temperature stability of TaN_x thin film resistor, temperature coefficient of resistance (TCR) was measured at different operation temperatures. Low-frequency current noise, i.e., flicker noise, was measured at frequency from 1 to 100K Hz. Finally, a two-ported S parameter measurement system at gigahertz level was utilized to investigate the stability of the TaN_x thin film resistor in radio frequency regime.

2. MATERIALS AND METHODS

6 inch single crystal, 4~7 μΩ-cm, (100)-oriented silicon wafers were used as the substrate in this study. All wafers were initially cleaned by a standard RCA process, and then a silicon oxide film of 500-nm in thickness was thermally grown at 1050 ^oC. 50-nm-thick TaN_x thin films were then deposited by a dc sputtering system (3308RDE, ULVAC, Japan). During the sputtering, argon and nitrogen were utilized as the reacting gases. To fabricate TaN_x thin films with various nitrogen compositions, different nitrogen flow ratios were employed in this experiment. The nitrogen flow ratio is defined as the proportion of nitrogen flow in the total gases during the sputtering. For example,

nitrogen flow ratio 5% is defined as the ratio of nitrogen partial flow to the total gas flow (nitrogen and argon) is 5%, and the deposited TaN_x film is denoted as TaN_x(5%). The dc power was maintained at 500 W, and the gas pressure was 6 mTorr during sputtering.

After TaN_x thin films were deposited, a 700-nm-thick photoresist was then coated using TEL Clean Track Model-MK8® system, followed by the resistor array with various dimensions were defined using the optical exposure systems (Canon FPA-3000i5 stepper, Japan). The helicon wave plasma ion etching system (ANELVA ILD-2100®, Japan) was then employed to etch the thin film resistor array. The power and pressure of the etching system were 2300 W and 12 mTorr, respectively. To obtain a better profile of the resistors, a bias of 90 V was also employed during etching process. Cl_2 and Cl_2/O_2 gas mixtures were used as the reactive gases of the plasma etching system. The total gas flow rate was maintained at 100 sccm during etching process.

Sheet resistance (R_s) of the TaN_x thin film was measured by a NAPSON® RT-80 4-point probe measurement system. X-ray diffractometer (XRD) was used for phase identification of the TaN_x thin films. The etching profiles of TaN_x thin films were observed using a scanning electron microscopy (SEM) system. Linewidth dependent R_s and TCR were measured by an Agilent 4156C semiconductor parameter analyzer. Low frequency noise was measured using Agilent 35670A dynamic signal analyzer and BTA 9812A noise analyzer at frequency ranging from 1 to 100 kHz. For RF characterization, the S-parameters were measured using Agilent 8510C network analyzer with the GGBs air coplanar probe (ACP) for ground-signal-ground (GSG) configuration.

3. RESULTS AND DISCUSSION

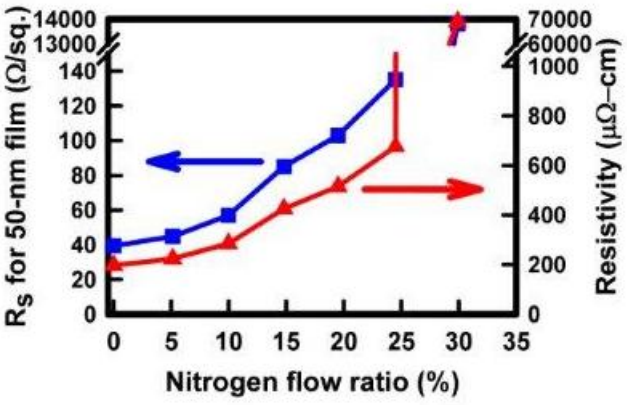

Figure 1. Resistivity and sheet resistance of the reactively sputtered TaN_x thin film as a function of nitrogen flow ratio.

Fig. 1 shows the resistivity and R_s of the TaN_x thin films as a function of the nitrogen flow ratio during reactive sputtering. The resistivity of TaN_x thin film increases slightly for the sample at nitrogen flow ratio from 0 to 25%, and then increases dramatically for the nitrogen flow ratio exceeding 25%. The R_s were also measured from a 50-nm TaN_x thin films using 4-point probe measurement method. The R_s ranging from 40 to 14000 μΩ/square is observed when increasing the

nitrogen flow ratio from 0 to 30%. The feature of wide-range in resistance of the TaN_x thin film by simply tuning the nitrogen flow ratio is a strong point for its application in thin film resistor.

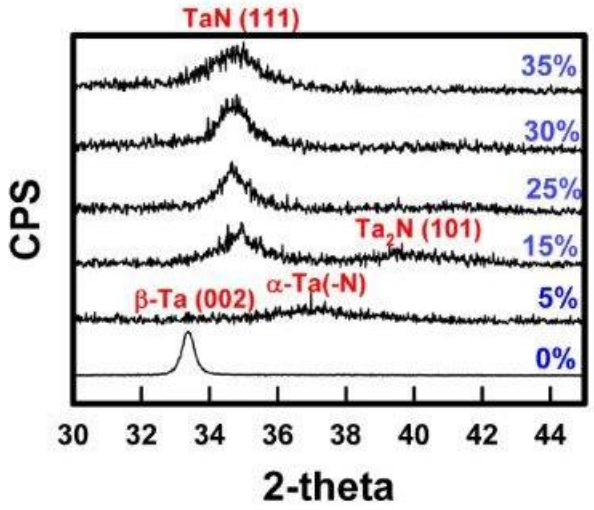

Figure 2. XRD spectra for the TaN_x films deposited at different nitrogen flow ratios.

Fig. 2 shows the XRD spectra for the TaN_x thin films deposited at various nitrogen flow ratios. The crystallographic structure of the TaN_x is strongly affected by the nitrogen flow ratio during sputtering. As seen in Fig. 2, the diffraction pattern taken from the pure Ta film, ie, 0% of the nitrogen flow ratio, can be indexed to β-Ta (tetragonal) phase. As the nitrogen flow ratio is increased to 5%, a weak □-Ta(-N) peak can be observed, indicating that the TaN_x(5%) is mainly composed of an amorphous-like Ta film with few nitrogen atoms doping. As to the flow ratio is increased to 15%, apparent NaCl-type TaN(111) and vague Ta_2N(101) peaks were observed in the deposited film. The intensity of Ta_2N(101) decreases upon increasing the nitrogen flow ratio, and TaN(111) peak dominates as the flow ratio is further increased up to 25%. In addition, the full width at half maximum (FWHM) of the TaN(111) peak is getting larger upon increasing the nitrogen flow ratio from 15 to 35%. Since the resistivity of TaN(111) and Ta_2N(101) phases are much larger than that of α-Ta(-N) phase, the resistivity of TaN_x film increases dramatically as the nitrogen flow ratio is exceed 10%, which is consistent to the result of Fig. 1.

To fabricate a high-quality thin film resistor, a high-precision lithography and plasma ion etching system were used to pattern the TaN_x thin film. In general, Cl_2 is often used as the reacting gas for Ta film etching, and a sharp profile can be obtained after the etching process. Fig. 3(a) shows the cross sectional SEM image of the TaN_x(5%) film by using Cl_2 plasma etching system. The etching selectivity of the Cl_2 plasma is, however, poor to silicon oxide substrate. The instability of the etching selectivity causes over-etching problem and may damage to other devices beneath the TaN_x resistor, as well as the degradation of high-frequency property of the device.

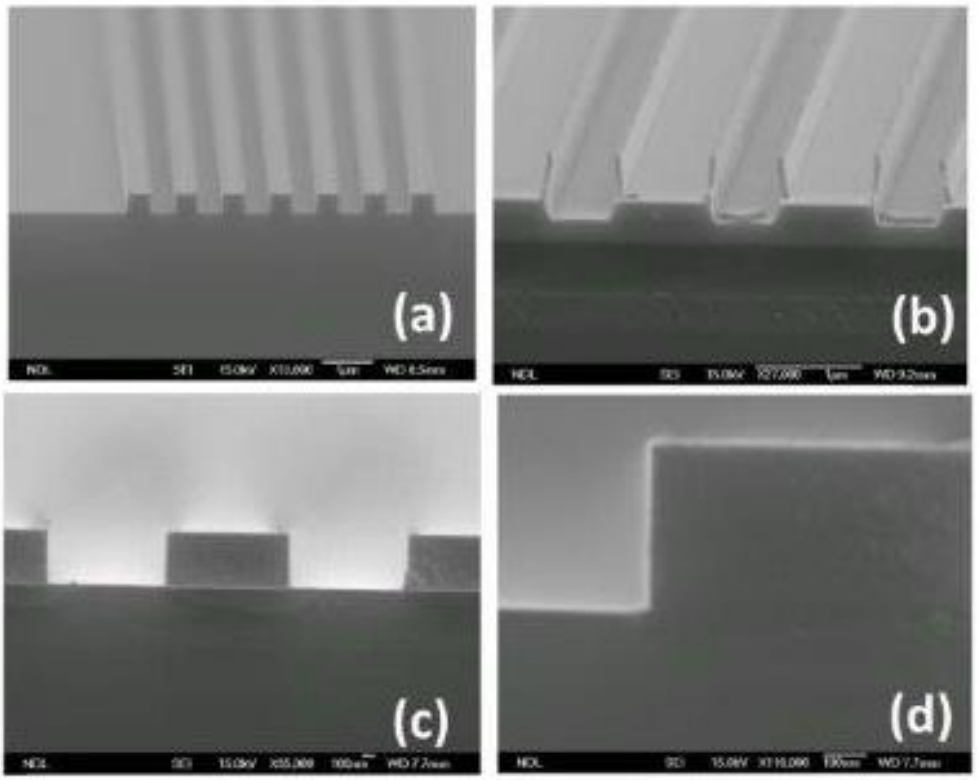

Figure 3. Cross-sectional SEM images of the TaN_x patterns by different etch parameters. (a) Cl_2, (b) Cl_2/O_2: 95/5 mixture, (c) and (d) two-step etching.

To improve the selectivity, an etching recipe of a Cl_2/O_2 = 95/5 sccm gas mixture was employed. It was found that increasing the flow of oxygen during etch process could much improve the selectivity, while decrease the etch rate rapidly. This is why only 5 sccm of oxygen gas is added in the etching system. Fig. 3(b) presents the etching profile of the TaN_x(5%) pattern using Cl_2/O_2 as the reacting gas. As seen in the figure, apparent by-product formed on the sidewall of the TaN_x thin film. This by-product has been analyzed by Auger electron spectroscopy, and is verified to be composed of Ta-C-O compound (not shown in this paper). This phenomenon, which is known as "fencing effect", is caused by the production of polymer from oxygen reaction during etching process.

Since it is not satisfied with the demand of both etching profile and selectivity for the thin film resistor, a navel two-step etch is proposed in this study. At first step, the TaN_x thin film was etched using pure Cl_2 gas to obtain a sharp profile and high etching rate, and next, a Cl_2/O_2 gas mixture was induced at the end of etching process to get a better selectivity. Figure 3(c) and (d) show the cross-sectional SEM images of the patterned TaN_x(5%) film using two-step etching. A sharp profile with high aspect ratio can be obtained using the two-step etching, as shown in the figure. We have tried to etch the TaN_x film with different nitrogen flow ratio, and the obtained results of etch profile and selectivity exhibit little difference with that of TaN_x(5%) film. The etching selectivity of TaN_x(5%) to silicon oxide film is measured to be 10, which is acceptable for the application of thin film resistor.

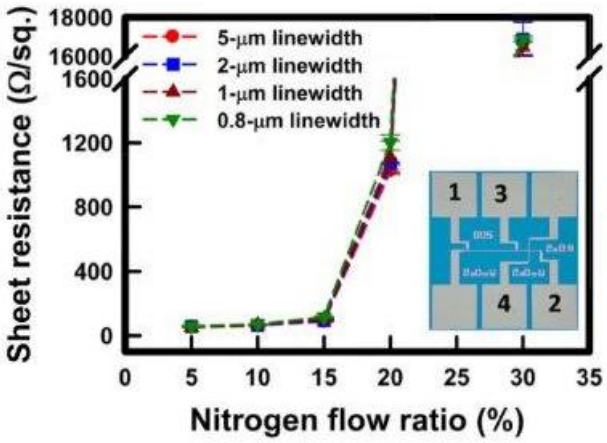

Figure 4. Sheet resistance of the TaN_x resistor as a function of nitrogen flow ratio. Inset shows the bridge structure for sheet resistance measurement.

Fig. 4 shows the R_s results of the TaN_x line patterns with various nitrogen flow ratios. The R_s results of the TaN_x thin film resistors show slightly increases at nitrogen flow ratio from 0 to 15%, and increases dramatically as the nitrogen flow ratio from 20 to 30%. In addition, the sheet resistances of TaN_x lines with different line-widths show invisible deviation, indicating that the two-step method is in well control and stable for pattering the TaN_x thin film resistors. In is also noted that, to accurately measure the resistance of TaN_x line, a bridge structure was employed in this measurement. Inset of Fig. 4 displays the optical microscope image of the bridge structure. As seen in the figure, pads 1 and 2 carry a constant current and pads 3 and 4 sense the voltage. Using the bridge structure, the parasitic resistances, contact resistance R_c and spread resistance R_{sp}, can be negligible because the voltage drops across them are very small due to a very tiny current is applied [13].

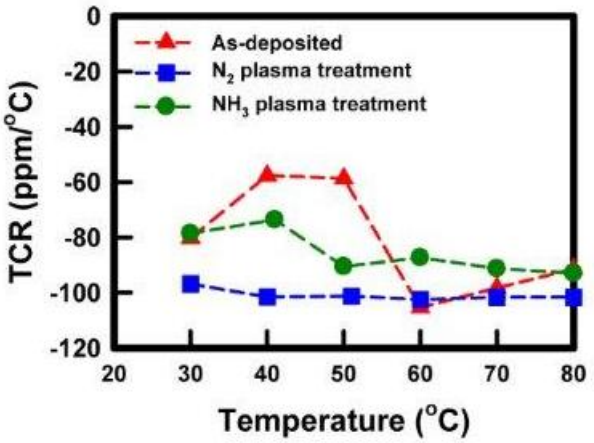

Figure 5. TCR properties of the TaN_x(5%) resistors as a function of measuring temperature.

To inspect the thermal noise related stability of the TaN_x thin film resistors, TCR was measurement at temperature ranging from 30 to 80 ^oC. The thermal noise is arisen from the random thermal motion of the charges in the thin film over the absolute temperature. Fig. 5 shows the TCR

properties of the TaN_x thin film resistors. The 5%nitrogen flow ratio of the TaN_x was chose because the resistivity range is suitable for TCR measurement and the pattern is stable. As shown in the figure, the temperature-induced resistance unstability is obvious for the as-deposited TaN_x(5%) thin film resistor. To improve TCR characteristic of the TaN_x thin film resistor, a post-deposited plasma treatment with different reacting gas was employed. The TCR of the TaN_x(5%) thin film resistor after NH_3 plasma treatment exhibits almost constant value, around -100 ppm/^oC, while N_2-plasma treated thin film resistor show a little vibration in the result.

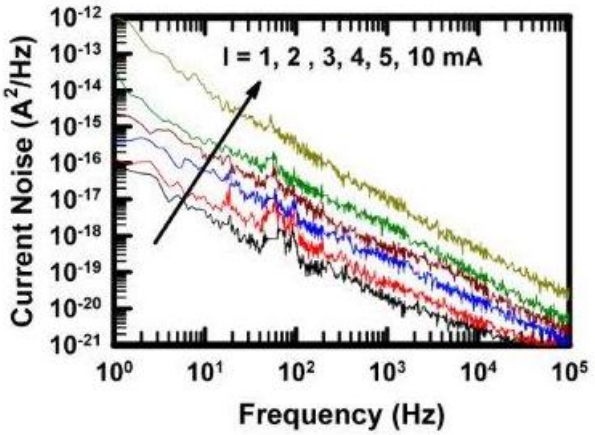

Figure 6. Current noise spectra of the TaN_x(5%) resistors at various applied currents.

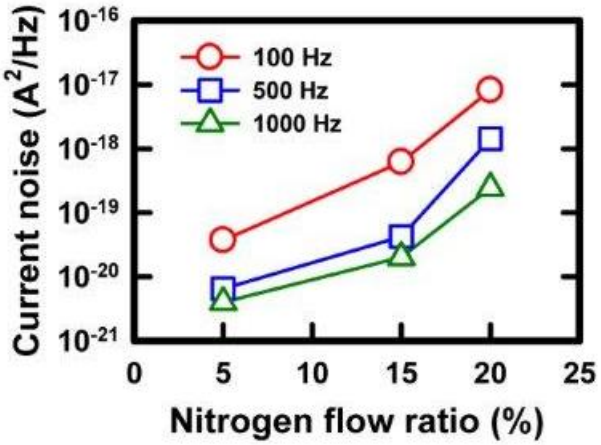

Figure 7. Current noise of the TaN_x thin film resistor as a function of the nitrogen flow ratio. The device is 15 μm in width and the applied current is 5 mA.

Fig. 6 shows the low frequency noise of the TaN_x(5%) thin film resistor. The measuring current applied to the resistor was ranging from 1 to 10 mA. At applied current ranging from 1 to 9 mA, the noise is inversely proportional to the frequency, exhibiting typical 1/f dependence. This phenomenon is the well-known 1/f noise or flicker noise. The flicker noise is originated from the current fluctuation of the condensed-matter materials of the devices [14]. When the applied current is increased to 10 mA,

the noise spectrum shows $1/f^{3/2}$ dependence. The $1/f^n$ (n>1) dependence is caused by electro-migration of the thin film resistor from the high applied current, which has been reported in literatures [15, 16]. Fig. 7 summarized the current noise results of the TaN_x(5%) thin film resistors at 5-mA applied current and specific frequency. It is visible that the current noise of TaN_x(5%) thin film resistor increases upon increasing the nitrogen flow ratio.

To evaluate high-frequency dependent resistance of the TaN_x thin film resistor, samples were also characterized using S-parameters at frequency ranging from 1 to 20 GHz. Left side of Fig. 8(a) shows the test structure of TaN_x thin film resistor, which uses a 3-ported ground-signal-ground configuration. To eliminate the parasitic impedance during high frequency measurement, a de-embedding structure, which is shown in the right side of Fig. 8(a), is employed in this analysis [17].

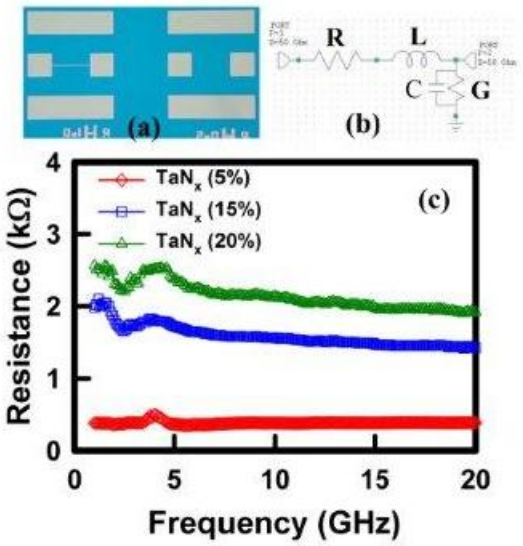

Figure 8. (a) Test structure and de-embedding of the TaN_x thin film resistors. (b) Schematic diagram of the telegrapher's transmission line model. (c) Resistances of the TaN_x resistors as a function of the measuring frequency.

The high-frequency dependent resistances were then extracted from the S-parameter results using a telegrapher's transmission line model [18], which is shown in Fig. 8(b). The telegrapher's transmission line equation can be expressed as:

$$[S]=\frac{1}{D_s}\begin{bmatrix}\left(Z^2-Z_0^2\right)\sinh\gamma\ell & 2ZZ_0\\ 2ZZ_0 & \left(Z^2-Z_0^2\right)\sinh\gamma\ell\end{bmatrix} \quad \text{.....(1)}$$

Where D_s=2*Z*Z_0 coshγl + (Z^2+Z_0^2)sinhγl ; Z_0 is the characteristic impedance of the measurement system; γ is the propagation constant; l is the length of the transmission line.

Using Equation 1, we can solve for γ and Z as functions of S-parameters:

$$e^{-\gamma\ell}=\left\{\frac{1-S_{11}^2+S_{21}^2}{2S_{21}}\pm K\right\}^{-1} \quad \text{.....(2)}$$

$$Z^2 = Z_0^2 \frac{(1+S_{11})^2 - S_{21}^2}{(1-S_{11})^2 - S_{21}^2} \quad \text{.....(3)}$$

Where

$$K = \left\{ \frac{\left(S_{11}^2 - S_{21}^2 + 1\right)^2 - (2S_{11})^2}{(2S_{21})^2} \right\}^{\frac{1}{2}} \quad \text{.....(4)}$$

Once γ and *Z* are known, from the standard transmission line relationships, the resistance of the thin film resistor can be determined:

R = *Re*{ γ*Z* }

Fig. 8(c) shows the extracted series resistances of the TaN_x thin film resistors as a function of the frequency. As seen in the figure, the resistances of the TaN_x(15%) and TaN_x(20%) samples decrease upon increasing the applied frequency, implying instable property of the TaN_x thin film resistor at radio frequency. On the other hand, the TaN_x(5%) thin film resistor exhibits a more stable performance even up to 20 GHz. The stable electrical performance at high frequency of the TaN_x(5%) thin film resistor indicates that it is more suitable for the high-precision thin film resistor at radio frequency regime.

4. CONCLUSION

TaN_x as the thin film resistor has been studied in this paper. As a concern of etching profile and selectivity, a novel two-step etching method was proposed to satisfy the demand of high-quality thin film resistor. The TaN_x the thin film resistor with NH_3 plasma treatment exhibits a stable temperature coefficient of resistance. As to the stability characteristic at low-frequency, the result shows that current noise of the thin film resistor increases upon increasing the nitrogen flow ratio. The resistance of TaN_x(5%) thin film resistor is stable even at radio frequency, indicating that it is more suitable for high-precision, integrated thin film resistor application at high frequency regime.

ACKNOWLEDGEMENTS

The authors would like to thank Taipei Medical University – Shuang Ho Hospital, and Ministry of Science and Technology, for financially supporting this research under contract nos. 103TMU-SHH-15 and NSC 102-2622-E-038-004-CC3.In addition, the authors are grateful to the National Nano Device Laboratories for their support in the fabrication process.

References

1. Y. Li, C. Wang, and N. Y. Kim, *Solid State Electron* 103 (2015) 147.
2. T. C. Tang and K. H. Lin, *Ieee T Comp Pack Man* 4 (2014) 648.
3. Y. C. Tseng and T. G. Ma, *Electron Lett* 48 (2012) 1605.
4. Y. S. Lin and J. H. Lee, *Ieee T Microw Theory* 61 (2013) 2594.
5. C. Y. Hung and M. H. Weng, *Ieee T Electron Dev* 59 (2012) 1164.
6. A. Ito, M. D. Church, C. S. Rhee, J. M. Johnston, J. T. Gasner, W. A. Ligon, P. A. Begley, and G.

A. Dejong, *Ieee T Electron Dev* 41 (1994) 1149.
7. V. Mathur and S. Vangala, *Ieee Photonic Tech L* 27 (2015) 141.
8. D. P. Zhu, X. Q. Lin, and L. Luo, *J Electron Packaging* 131 (2009) 011006.
9. Y. M. Lu, R. J. Weng, W. S. Hwang, and Y. S. Yang, *Materials Chemistry and Physics* 72 (2001) 278.
10. A. Scandurra, G. F. Indelli, B. Pignataro, S. Di Marco, M. A. Di Stefano, S. Ravesi, and S. Pignataro, *Surf Interface Anal* 40 (2008) 758.
11. S. M. Kang, S. G. Yoon, S. J. Suh, and D. H. Yoon, *Thin Solid Films* 516 (2008) 3568.
12. A. Mellberg, S. P. Nicols, N. Rorsman, and H. Zirath, *Electrochem Solid St* 7 (2004) G261.
13. A. Lalany, R. T. Tucker, M. T. Taschuk, M. D. Fleischauer, and M. J. Brett, *J Vac Sci Technol A* 31 (2013) 031502.
14. S. Grover, S. Dubey, J. P. Mathew, and M. M. Deshmukh, *Applied Physics Letters* 106 (2015) 051113.
15. S. Samanta, K. Das, and A. K. Raychaudhuri, *Nanoscale research letters* 8 (2013) 165.
16. C. Ciofi and B. Neri, *J Phys D Appl Phys* 33 (2000) R199.
17. B. Han, T. S. Zhou, X. M. Xu, P. L. Li, M. Cai, J. F. Huang, and J. J. Gao, *Int J Electron* 100 (2013) 637.
18. L. F. Tiemeijer, R. M. T. Pijper, and W. van Noort, *Ieee T Microw Theory* 57 (2009) 1581